Colloids and Surfaces A: Physicochem. Eng. Aspects 481 (2015) 314–318

Contents lists available at ScienceDirect

Colloids and Surfaces A: Physicochemical and Engineering Aspects

journal homepage: www.elsevier.com/locate/colsurfa

VO_2(B) @ carbon cathodes for lithium ion batteries

V.S. Reddy Channu [a,*], B. Rambabu [b], Kusum Kumari [c], Rudolf Holze [d]

[a] SMC Corporation, College Station, TX 77845, USA
[b] Solid State Ionics and Surface Sciences Lab, Department of Physics, Southern University and A&M College, Baton Rouge, LA 70813, USA
[c] Department of Physics, National Institute of Technology, Warangal, India
[d] Institut für Chemie, AG Elektrochemie, Technische Universität Chemnitz, D-09107 Chemnitz, Germany

HIGHLIGHTS

- Carbon coated VO_2(B) nanostructures were synthesized for electrodes in lithium ion batteries by hydrothermal method.
- The diffraction spots can be indexed to monoclinic structure of VO_2(B).
- Carbon coated VO_2(B) without H_2 gas electrodes have higher discharge capacity than the carbon-coated VO_2(B) electrodes in H_2 gas.
- Reaction under H_2 gas more economical in production of more carbon from sucrose.

GRAPHICAL ABSTRACT

TEM image of VO_2(B)@C.

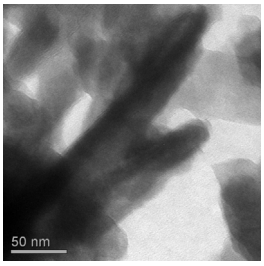

ARTICLE INFO

Article history:
Received 26 December 2014
Received in revised form 24 April 2015
Accepted 10 May 2015
Available online 6 June 2015

Keywords:
Carbon
Vanadium oxide
Cathode
H_2 gas effect
Lithium ion battery

ABSTRACT

Carbon coated vanadium oxide nanostructures were synthesized from the vanadium oxide sol using hydrothermal method with and without H_2 gas atmosphere for the purpose of cathodes in the lithium-ion batteries. The synthesized materials were characterized using x-ray diffraction (XRD) and transmission electron microscopy (TEM). A TEM image shows the thickness of carbon coating is more on vanadium oxide under H_2 gas atmosphere during synthesis. Electrochemical results shows that carbon coated vanadium oxide without H_2 gas atmosphere have higher capacity than the carbon coated vanadium oxide electrode with H_2 gas atmosphere.

1. Introduction

Cathodes are very essential and a significant part of lithium-ion batteries (LIBs), and excessive research efforts have been dedicated to cathode materials in order to decrease costs and to address safety issues [1]. For Li-ion battery applications, vanadium oxides are an attractive alternative, as vanadium is known to exist in a wide range of oxidation states from +2, as in VO, to +5, as in V_2O_5, and the vanadium oxides have the prospective to offer much higher capacities along with the important benefits of low cost, abundant source material, and easy synthesis. Over the years, vanadium oxides have involved special interest because of their owing structural flexibility combined with their interesting chemical and physical properties for electrochemical and catalytic applications [2]. Among the various known vanadium oxides, metastable oxides such as V_2O_5, $H_2V_3O_8$, VO_2(B), and LiV_3O_8 have been found to show fascinating cathode properties in lithium cells [3–6]. VO_2 reveals four different polymorphic structures, counting the most stable VO_2(R) with rutile structure, the monoclinic VO_2(R) with a slightly distorted rutile structure, the tetragonal structure of VO_2(A), and

* Corresponding author.
E-mail address: chinares02@gmail.com (V.S.R. Channu).

http://dx.doi.org/10.1016/j.colsurfa.2015.05.035
0927-7757/

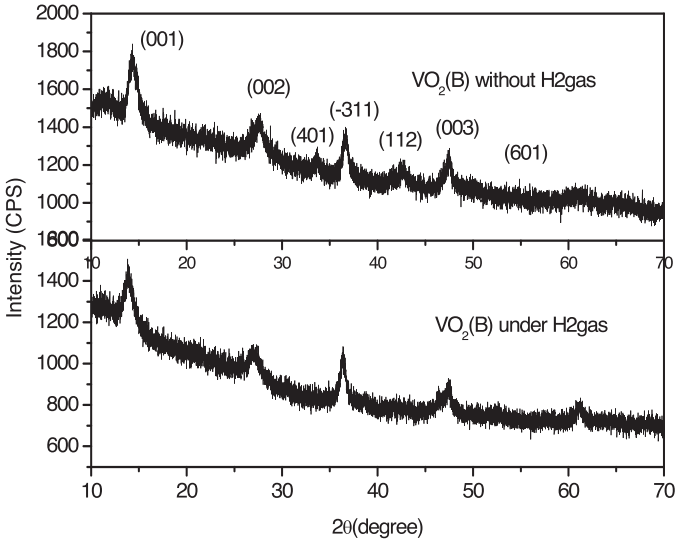

Fig. 1. XRD patterns of VO_2(B)@ C.

the metastable VO_2(B) with monoclinic structure [7]. VO_2(B), in particular, with its metastable monoclinic structure, is a favorable cathode material for both organic and aqueous lithium-ion batteries [8,9]. The crystal structure of VO_2(B) consists of sheets of edge sharing VO_6 octahedral linked by corner sharing to adjacent sheets along the c-direction of the unit cell [10]. This sharing structure is related to the structural stability and the subsequent resistance to lattice shearing during cycling in the lithium-ion battery [11]. Lately, significant efforts have been through in the direction of the preparation of VO_2(B) nanostructures. Quite a few nanostructured VO_2(B) materials, including nanoribbons, nanowires, nanorods, nanobelts, nanoneedles, and urchin-like morphologies have been obtained [12–14]. Nevertheless, its poor cycling lifetime (usually less than 20 cycles) significantly limits practical applications. The capacity fading of nanostructure VO_2(B) is maybe due to vanadium dissolution as in other polymorphs below a discharge voltage of 2 V [15,16] and also the nanosized forms of VO_2(B), which have large specific surface areas and high surface energies, making it easier to form the agglomerated state during the electrochemical cycling, thus increasing the charge transfer resistance [17–19].

Lately, material scientists have revealed that coating the surface of the electrode material with carbon has been proven to be an effective way to increase the cycling stability [20–23]. The detailed mechanism responsible for this improvement remains unclear; one possible explanation is the enhanced electronic conductivity resulting from the carbon layer [24,25].

Motivated by this concept, we have synthesized a novel VO_2(B) by carbon coated with and without H_2 gas to know the effect of amount of carbon deposition on electrochemical properties. The controlled synthesis of VO_2(B) is relatively difficult because vanadium is known to exist in a wide range of oxidation states from +2 to +5, and VO_2(B) tends to be transformed (>300 °C) to thermodynamically more stable rutile VO_2 [25], which is not usable as a cathode material for the lithium-ion battery. The electrochemical measurements demonstrate that the carbon coated nanostructure without H_2 gas can be used as an alternative cathode material in lithium-ion batteries with high capacity, good cycling stability, and high-rate capability.

2. Experimental

1.33 g of V_2O_5 powder was slowly dissolved in 100 mL aqueous hydrogen peroxide (33%) solution. A transparent orange solution

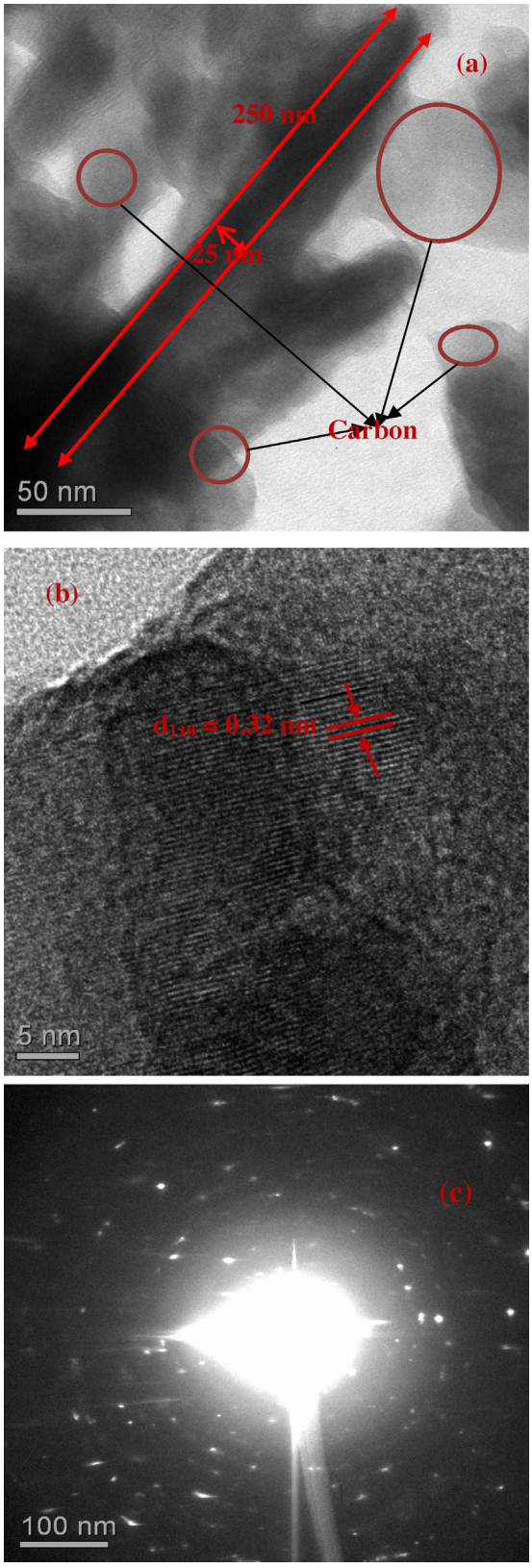

Fig. 2. TEM and HRTEM and SAED images of VO_2(B)@C without H_2 gas.

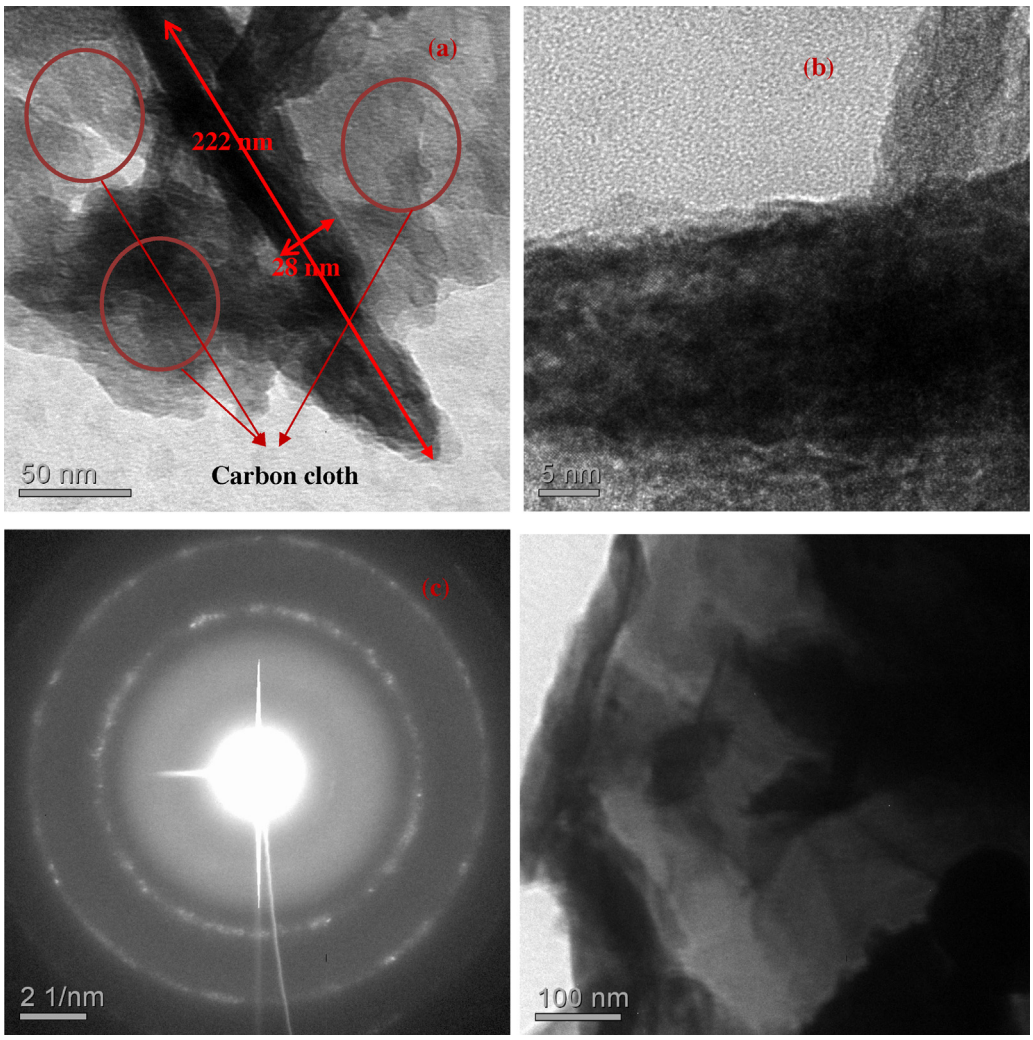

Fig. 3. (a–c) TEM and HRTEM and SAED images of VO_2(B)@C under H_2gas. (d) TEM image of carbon cloth.

was formed after V_2O_5 was completely dissolved. The orange-colored gel was redispersed in 200 mL water and aged for 15 days at room temperature. 0.1 g of sucrose was dissolved in 100 mL of aged gel and then transferred into a glass jar in an autoclave, kept at 180 °C for 24 h with (under) and without H_2 gas atmosphere and cooled at room temperature. The final product washed several times with distilled water and C_2H_5OH followed by vacuum dried at 100 °C over night.

Crystallographic information on the samples was obtained using a X-ray powder diffractometer STADI P (STOE) with Ge(111) monochromatized Cu Kα radiation (λ = 1.54187 Å). Diffraction data were collected over the 2θ range from 10° to 70°. The morphologies of the resulting products were characterized using a transmission electron microscopy (Philips CMG 200 FEG) (TEM).

The electrode for cycling tests were prepared by mixing 80 wt.% active material with 10 wt.% polyvinylidene fluoride (PVDF) binder and 10 wt.% acetylene black in α-terpineol; the mixture was painted on 1 cm-diameter circular stainless – steel mesh and kept at 100 °C over night under vacuum. The dried electrodes were pressed by applying 0.5 tons of pressure on a stainless steel (SS) mesh. Typical electrode mass and thickness were 5–10 mg and 0.04–0.08 mm. The electrolyte was 1 M $LiPF_6$ in a mixture of ethylene carbonate (EC), diethyl carbonate (DEC) and dimethyl carbonate (DMC) (1:1:1 by volume, provided by Merck). Cells were fabricated in an argon-filled glove bag and galvanostatically cycled with a current density 50 mA/g and 100 mA/g over a voltage range 1.5–4 V vs. Li/Li^+ with a Wuhan Land CT 2001A cycler at 25 °C.

3. Results and discussion

Fig. 1 shows XRD patterns of VO_2(B) with and without H_2 gas. All the diffraction peaks can be indexed with standard JCPDS (# 31-1438) of monoclinic with cell parameters of a = 12.03 Å, b = 3.693 Å and c = 6.42 Å. Better crystallinity observed in VO_2(B) without H_2 gas compared to VO_2(B) under H_2 gas, this may be due to less amorphous carbon coating on the surface of the nanomaterials. Carbon is not detected in the pattern of VO_2(B)@C composites with and without H_2 gas. Carbon obtained from sucrose under hydrothermal condition is amorphous and cannot be detected by XRD even with higher amounts [20]. Sizes of the VO_2(B) without H_2 gas and with H_2 gas nanostructures crystallites were estimated using the Scherrer formula [$\tau = K\lambda/\beta\cos\theta$]. Where τ is the mean size of the ordered (crystalline) domains, which may be smaller or equal to the grain size; K is a dimensionless shape factor, with a value close to unity. The shape factor has a λ is the X-ray wavelength (1.54); β is the line broadening at half the maximum intensity (FWHM), after subtracting the instrumental line broadening, in radians. This quantity is also sometimes denoted as Δ (2θ); θ is the Bragg angle.

The calculated D-spacing is 5.81 Å for VO_2(B) nanorods, 5.10 Å for carbon coated VO_2(B) nanostructures with H_2 gas, and 5.15 Å

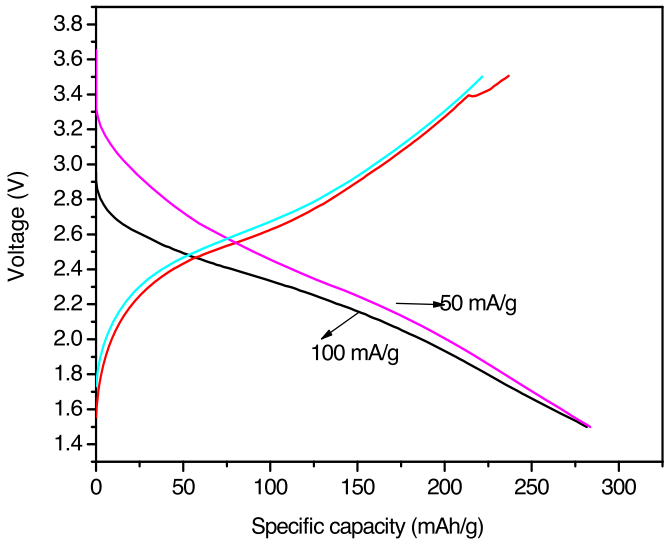

Fig. 4. Charge–discharge profiles of VO_2(B)@C without H_2 gas cathode.

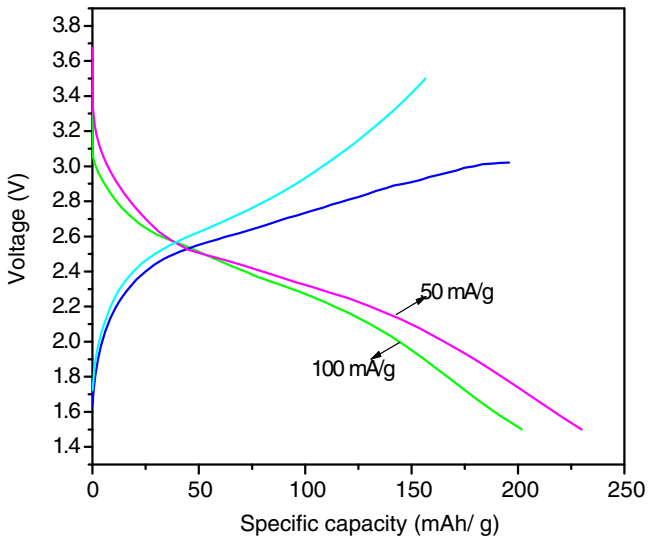

Fig. 5. Charge–discharge profiles of VO_2(B)@C under H_2 gas cathode.

carbon coated VO_2(B) nanostructures under H_2 gas at (200) plane. The difference between the calculated D-spacing is 0.71 Å of VO_2 (B) nanorods and carbon coated VO_2 (B) nanostructures without H_2 gas, whereas 0.66 Å of VO_2 (B) nanorods and carbon coated VO_2 (B) nanostructures under H_2 gas.

Fig. 2a shows the TEM image of VO_2 (B)@C without H_2 gas. After carbon coating process without H_2 gas, the sample consist of well-defined nanorods with length up to several micrometers, and the difference rating between cores and shells could even be observed, representing that each VO_2(B) core is encapsulated into amorphous carbon shell, which is similar to carbon coated Fe_3O_4 [20]. The thickness of the carbon shell can be controlled by the hydrothermal reaction time and the quantity of sucrose and atmosphere inside the auto clave.

The high-resolution HRTEM image of an individual VO_2 (B)@C nanorod without H_2 gas shown in Fig. 2(b) visibly exhibits lattice fringes and covered by amorphous carbon coating, where the lattice planes with a d spacing of 0.35 nm correspond to the (1 1 0) planes, which is a good match to monoclinic VO_2(B) (JCPDS No: 31-1438), it was confirmed by XRD. The selected-area electron diffraction (SAED) pattern (Fig. 2c) was recorded from the individual nanorod region of Fig. 2(a), demonstrating that the synthesized nanorods are single-crystal with preferential growth along the [0 1 0] direction.

TEM images of carbon coated vanadium oxide (Fig. 3a) under H_2 gas show nanostructures covered by thick carbon cloth. A single nanobar identified with dimensions of 222 nm length and 28 nm diameter. Low crystallinity and carbon cloth coverage on vanadium oxide nanostructures can be clearly seen in HRTEM image (Fig. 3b). The selected area electron diffraction pattern of a single nanostructure is shown in Fig. 3c. A monoclinic structure of vanadium oxide nanostructure can be indexed by the diffraction spots in Fig. 3c. Fig. 3d shows TEM image of carbon. We can conclude carbon deposition on vanadium oxide by comparing Fig. 2a and Fig. 3b and d.

Fig. 4 shows the charge-discharge profiles of the VO_2(B)@C without H_2 gas cathode at 50 mA/g and 100 mA/g current densities. The initial discharge capacities are 282 mAh/g at 50 mA/g and 283 mAh/g at 100 mA/g current density. The initial charge capacities are 237 mAh/g at 50 mA/g and 222 mAh/g at 100 mA/g current density. The columbic efficiencies are 84% at 50 mA/g and 79% at 100 mA/g. The charge–discharge curves of the VO_2 (B)@C under H_2 gas cathode at 50 mA/g and 100 mA/g current densities are shown in Fig. 5. The initial discharge capacity is

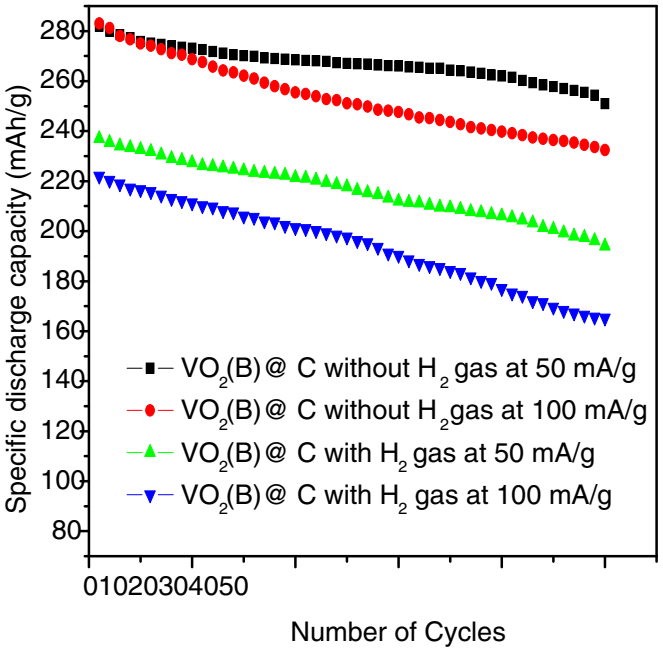

Fig. 6. Cycling performance of VO_2(B)@C cathode.

230 mAh/g at current density 50 mA/g, and charge capacity is 157 mAh/g, the columbic efficiency is 68%. The initial discharge capacity at a current density of 100 mA/g is 202 mAh/g, and charge capacity is 196 mAh/g, the columbic efficiency is 97%. The initial discharge capacities of VO_2(B)@C is much higher than the VO_2(B) nanorods (150 mAh/g) and VO_2(B)@C core–shell microspheres (187 mAh/g), VO_2(B) –multiwal carbon nanotubes (MWCNT) (177 mAh/g) [13,21,26].

Fig. 6 shows cycling performance of VO_2(B)@C nanostructures with and without H_2 gas treatment cathodes.

4. Conclusions

Carbon coated vanadium oxide nanostructures successfully synthesized using vanadium oxide sol and sucrose through hydrothermal method with and without H_2 gas atmosphere. Sucrose is a cheap and environmentally friendly reagent. During the synthe-

sis, sucrose act as reductant and carbon source, without adding unfamiliar surfactants or hazard reducing reagents. The synthetic approach has the merits of easy, low-cost, convenience and environmentally benign. If the reaction performed under H_2 gas then more amount carbon can produce, this will be useful in large scale production materials to minimize the cost of the material. TEM images shows that high thickness of carbon-coated vanadium oxide nanostructures under H_2 gas. Electrochemical studies show that the carbon coated vanadium oxide nanostructures without H_2 gas have higher discharge capacity than the carbon coated vanadium oxide nanostructures under H_2 gas.

Acknowledgement

One of the authors (VSRC) thanks the Alexander von Humboldt-Foundation for a fellowship. The authors gratefully acknowledge valuable contributions by M. Schlesinger and M. Mehring in the structural analysis using XRD and support by Dr. Steffen Schulze during SEM and TEM characterization.

References

[1] X. Xu, S. Lee, S. Jeong, Y. Kim, J. Cho, Mater. Today 16 (2013) 487.
[2] C. Wu, F. Feng, Y. Xie, Chem. Soc. Rev. 42 (2013) 5157.
[3] D. Su, G. Wang, ACS Nano 7 (2013) 218.
[4] Q. An, J. Sheng, X. Xu, Q. Wei, Y. Zhu, C. Han, C. Niu, L. Mai, New J. Chem. 38 (2014) 2075.
[5] L. Mai, Q. Wei, Q. An, X. Tian, Y. Zhao, X. Xu, L. Xu, L. Chang, Q. Zhang, Adv. Mater. 25 (2013) 2969.
[6] A. Pan, J. Liu, J.G. Zhang, G. Cao, W. Xu, Z. Nie, X. Jie, D. Choi, B.W. Arey, C. Wang, S. Liang, J. Mater. Chem. 21 (2011) 1153.
[7] S. Rao Popuri, M. Miclau, A. Artemenko, C. Labrugere, A. Villesuzanne, M. Pollet, Inorg. Chem. 52 (2013) 4780.
[8] S.A. Corr, M. Grossman, Y. Shi, K.R. Heier, G.D. Stuckya, R. Seshadri, J. Mater. Chem. 19 (2009) 4362.
[9] S. Ni, H. Zeng, X. Yang, J. Nanomaterials 2011 (2011) 1.
[10] E. Baudrin, G. Sudant, D. Larcher, B. Dunn, J.M. Tarascon, Chem. Mater. 18 (2006) 4369.
[11] C. Tsang, A. Manthiram, J. Electrochem. Soc. 144 (1997) 520.
[12] L. Mai, X. Xu, L. Xu, Ch. Han, Y. Luo, J. Mater. Res. (2011) 1.
[13] Ch.V. Subba Reddy, E.H. Walker Jr., S.A. Wicker, Q.L. Williams, R.R. Kalluru, Curr. Appl. Phys. 9 (2009) 1195.
[14] W. Jiang, J. Ni, K. Yu, Z. Zhu, Appl. Surf. Sci. 257 (2011) 3253.
[15] G. Sudant, E. Baudrin, B. Dunn, J.M. Tarascon, J. Electrochem. Soc. 151 (2004) A666.
[16] N.A. Chernova, M. Roppolo, A.C. Dillon, M.S. Whittingham, J. Mater. Chem. 19 (2009) 2526.
[17] G. Armstrong, J. Canales, A.R. Armstrong, P.G. Bruce, J. Power Sources 178 (2008) 723.
[18] H.M. Liu, Y.G. Wang, K.X. Wang, E. Hosono, H.S. Zhou, J. Mater. Chem. 19 (2009) 2835.
[19] S. Rahul, R. Oscar, R.S. Katiyar, J. Renew. Sust. Energy 1 (2009) 023103.
[20] V.S. Reddy Channu, D. Ravichandran, Rudolf Holze, B. Rambabu, Appl. Surf. Sci. 305 (2014) 596.
[21] M.M. Rahman, J.Z. Wang, N.H. Idris, Z. Chen, H. Liu, Electrochim. Acta 56 (2010) 693.
[22] Y. Zhang, Ch. Chen, J. Zhang, L. Hu, W. Wu, Y. Zhong, Y. Cao, X. Liu, Ch. Huang, Curr. Appl. Phys. 13 (2013) 47.
[23] Q. Zhao, L. Jiao, W. Peng, H. Gao, J. Yang, Q. Wang, H. Du, L. Li, Z. Qi, Y. Si, Y. Wang, H. Yuan, J. Power Sources 199 (2012) 350.
[24] C.H. Mi, Y.X. Cao, X.G. Zhang, X.B. Zhao, H.L. Li, Powder Technol. 181 (2008) 301.
[25] A.M. Kannan, A. Manthiram, Solid State Ionics 159 (2003) 265.
[26] F. Wang, Y. Liu, C.Y. Liu, Electrochim. Acta 55 (2010) 2662.